

## Chapter 6

# Attribution of Sulfur and Visibility Impairment

### 6.1 Introduction

The aerosol attribution component of WHITEX was designed to evaluate the feasibility of attributing single source emissions (for purposes of this experiment, NGS emissions) to ambient aerosol concentrations at a number of receptor sites. The primary receptor sites were Grand Canyon and Canyonlands National Parks and Glen Canyon National Recreation Area (Page). The WHITEX study region is shown in Figure 6.1. Figures 6.1a and b show in three-dimensional perspective the WHITEX study region and the smaller Grand Canyon/Page area. Key monitoring sites, topographic features, and emission sources are shown.

Several quantitative and qualitative analysis techniques are used to gain insight into the performance of each individual modeling approach. The analysis include:

- Emissions. The relative source strength of NGS compared to other sources in the region and the location of NGS and other regional emissions relative to key receptor sites.
- Trajectory and streakline analysis. The probability that the predicted presence of NGS or other source emissions is coincident with elevated ambient sulfur concentrations or is due to random mechanisms is examined.
- Spatial and temporal patterns in visibility reducing aerosol concentrations. Spatial patterns in aerosol concentrations as a function of time are examined qualitatively and quantitatively through empirical orthogonal function analysis.
- Tracer mass balance regression. As a special case of the general mass balance (GMB) equation the variation of sulfur and natural or artificial tracers as a function of time are used to attribute emissions.
- Differential mass balance. As a second special case of the GMB formalism, the spatial variation of the unique tracer,  $CD_4$ , is used to estimate dispersion while deposition and conversion are explicitly calculated.
- Chemical mass balance. As a third special case of GMB the chemical mass balance formalism is used to estimate source contribution of primary aerosol species and to set an upper bound on NGS contributions. Several alternative approaches for attributing secondary aerosols are explored.

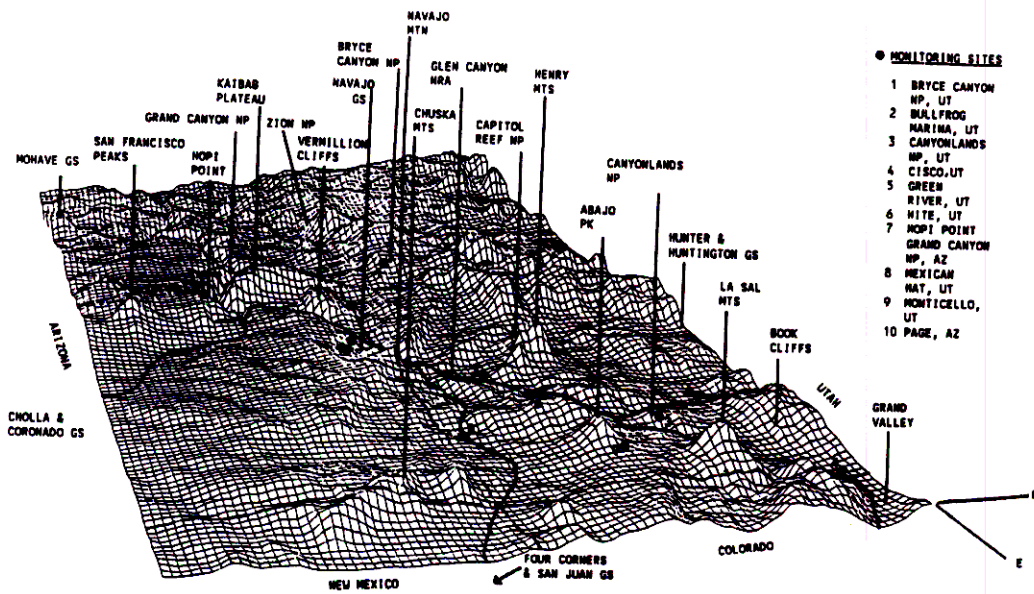


Figure 6.1: a. Three dimensional perspective of the WHITEX study region.

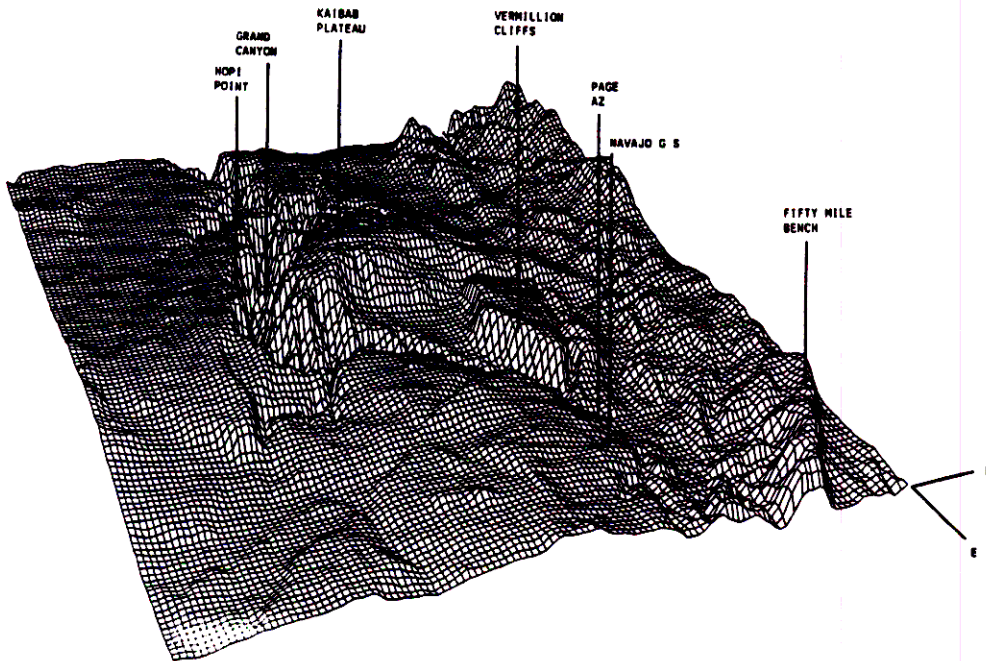


Figure 6.1: b. Three dimensional perspective of the Grand Canyon/Page area.

In Section 6.2.1, regional patterns in emissions of sulfur dioxide in the WHITEX study and surrounding area are explored. In Chapter 4 a significant portion of data gathered during the WHITEX study and all data used in analysis are presented. In Section 6.3 a literature review of oxidation and deposition rates for various gas and particle species is reviewed. Section 6.4 presents the trajectory and streakline analysis, while Section 6.5 explores the spatial and temporal sulfate sulfur trends. Subsections of Section 6.5 are used to look at sulfate time histories, explore sulfate spatial patterns and present the results of an empirical orthogonal function analysis. Section 6.6 presents the quantitative calculations of estimated source contribution to ambient aerosol species. First, all mass balance equations are combined into a general mass balance formalism (GMB). Then special cases of GMB are used to attribute sulfur dioxide and sulfate sulfur to various sources including NGS. The GMB formalism as well as the special cases analysis of tracer mass balance regression, differential mass balance and chemical mass balance are presented in Appendices 6A, 6B, 6C, and 6D. Also included in the appendices for each special attribution approach are model assumptions, potential deviations from assumptions, model input data, model outputs, and discussion of uncertainty analysis. Section 6.6.1, 6.6.2, and 6.6.3 presents the attribution results along with uncertainties using the tracer mass balance, differential mass balance and chemical mass balance techniques, respectively. Tracer mass balance examines the variation in secondary aerosol species as a function of trace material concentration as a function of time while chemical mass balance looks at the relative ratios of tracers at one point in time. Differential mass balance uses the unique tracer to estimate dispersion while aerosol deposition and gas to aerosol oxidation rates are explicitly calculated. Streakline analysis is used to estimate plume age, one variable used in the DMB calculation. Section 6.7 presents the apportionment of light extinction.

## 6.2 Emissions

Ambient aerosol concentrations and resulting visibility impairment are the result of emissions of precursor species to the atmosphere and subsequent atmospheric transport, dispersion, chemical reaction, and deposition. Emissions are the first link of a long and complex chain of events that determine the aerosol concentrations at any location.

### 6.2.1 Regional Emissions of $SO_2$ and $NO_x$

In the western United States there are numerous sources of anthropogenic emissions of  $SO_2$ ,  $NO_x$ , and particulates; including urban source areas as well as point sources. Sulfate spatial and temporal trends throughout the WHITEX study area may be influenced by the regional  $SO_2$  patterns. Therefore, a brief description of  $SO_2$  source strength and emissions will be presented.

NGS constitutes a large portion of the  $SO_2$  emitted within 300 km of NGS. Figure 6.1 shows the other large  $SO_2$  emission sources within this range. On an annual basis, the sources include Navajo at 163 tons/day, followed by San Juan at 115.6 tons/day, Four Corners at 105.5 tons/day, Mohave at 51.5, Huntington Canyon at 32.6, Cholla at 44.7, Coronado at 17.5, and Hunter at 15.9. However, most of these power plants are greater than 200 km from NGS.

The NGS power plant was operating continuously, if not uniformly, through out the WHITEX study period. Figure 6.2 shows the power generation as a function of time from Julian day 5 to Julian day 47 of 1987. The three-unit plant was run at times at its maximum capacity (2250 MWe); however, much of the time one unit was not operating, and during two days (Julian days 38-40) two units were not operating. The average power generated during the WHITEX period was 1787 MWe, 79 percent of rated maximum capacity.

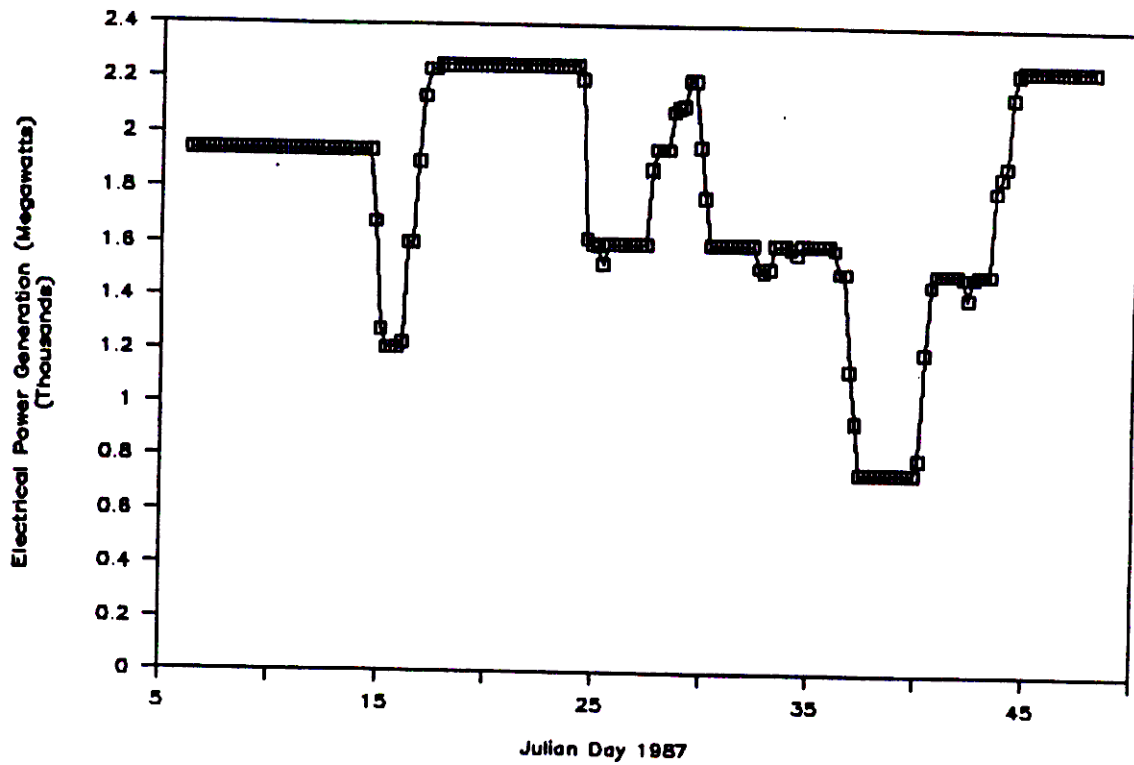


Figure 6.2: Power generated by the Navajo Generating Station during the WHITEX experiment.

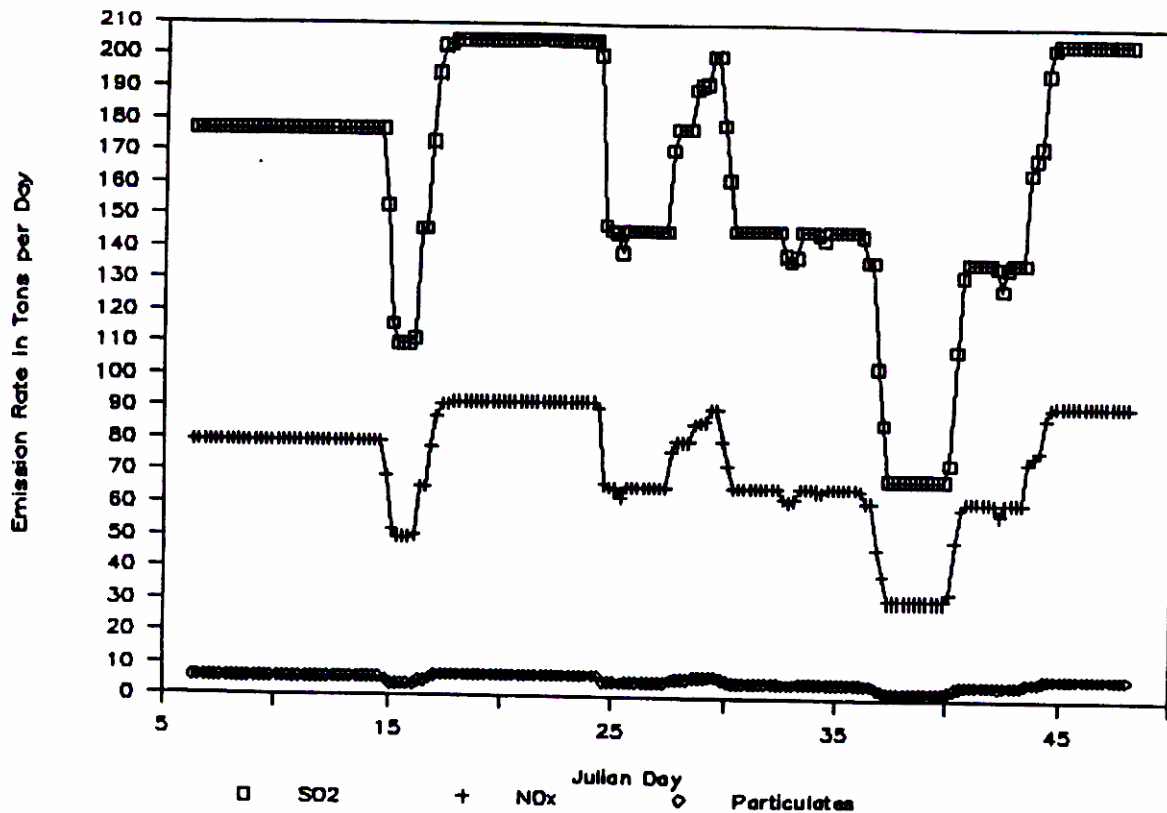


Figure 6.3: Emission rates of sulfur dioxide ( $SO_2$ ), nitrogen oxides ( $NO_x$ ), and particulates from the Navajo Generating Station during the WHITEX experiment.

Figure 6.3 shows the NGS  $SO_2$ ,  $NO_x$ , and particulate emissions calculated from power plant load information. These emissions were based on NGS performance tests in 1981 and May 1985 and are based on the following emission rates:  $SO_2$ , 0.75 pound per million Btu;  $NO_x$ , 0.34; and particulate, 0.02. The average emission rates from NGS over the WHITEX study period were calculated to be 163 tons per day for  $SO_2$ , 73 tons per day for  $NO_x$ , and 6.4 tons per day for particulates.

The closest sources of  $SO_2$  emissions other than coal fired power plants are the smelters in southern Arizona and Mexico. The three Arizona smelters operating during the WHITEX study are Asarco-Hayden, Inspiration, and Magma at San Manuel. The smelter at Douglas operated by Phelps Dodge ceased operations in January of 1987. By the consent decree governing the Douglas smelter the last day it could be operated was January 14. While the remaining Arizona smelters have controls on their emissions, Magma was only achieving 65 percent control in 1986 and 1987. During the WHITEX study period the Magma smelter was a formidable source with releases on the order of several hundred tons of  $SO_2$  per day.

The Mexican smelter at Nacozari came on line before the Douglas smelter ceased operations, essentially negating any benefits derived from shutting down the Douglas smelter. The Nacozari smelter is capable of emitting 1150 metric tons per day of  $SO_2$  through a 932 foot stack if no controls are utilized and the plant is at full capacity. Today, the Nacozari smelter has controls on its emissions capable of achieving over 90 percent control; however, during the WHITEX study it was uncontrolled. Another Mexican copper smelter, Cananea, located adjacent to Nacozari operated with no controls during the WHITEX period.

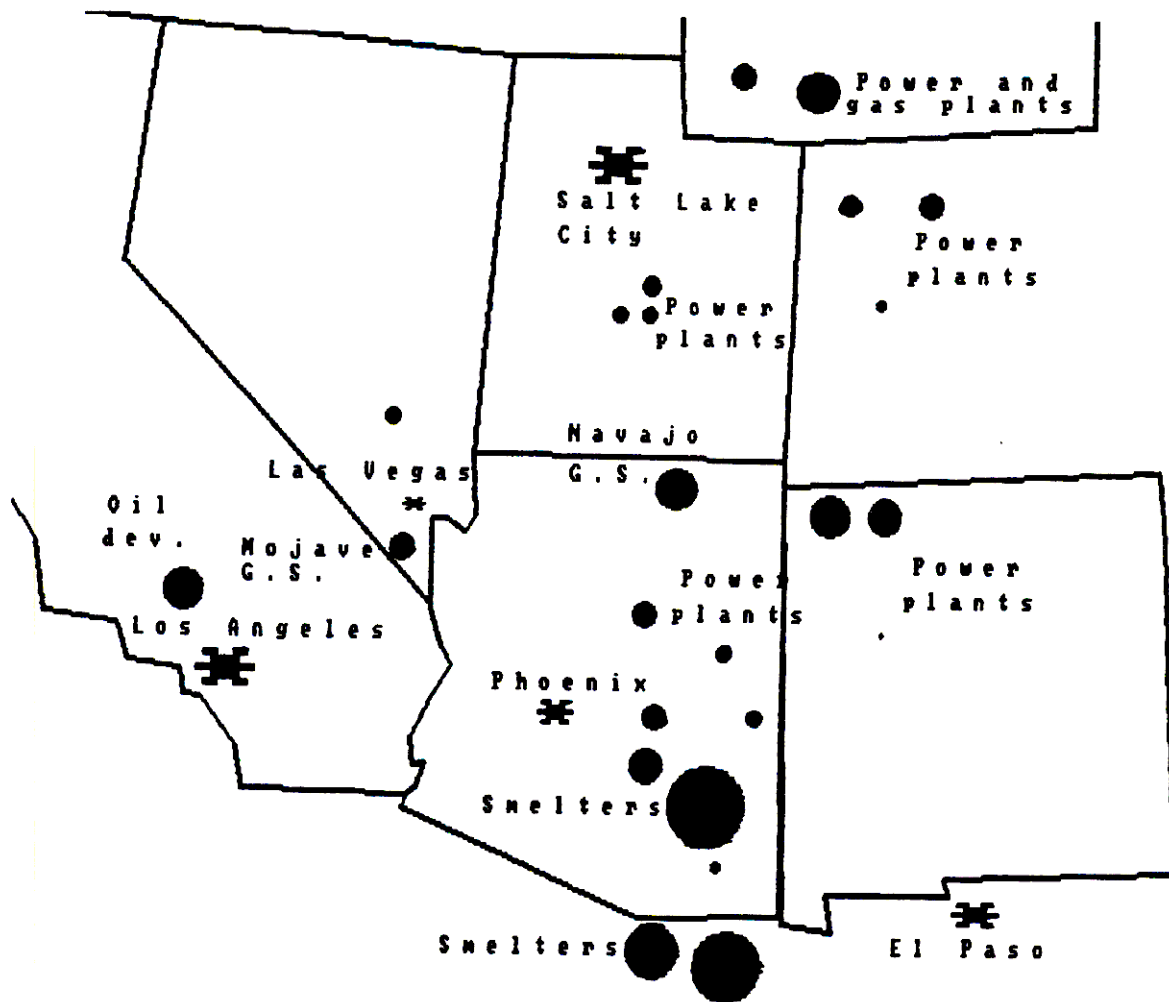


Figure 6.4: Approximate  $SO_2$  emissions from major point sources and urban areas in the southwest United States for 1987.

Table 6.1 details the best estimates of emissions from coal fired power plants, smelters, and other major  $SO_2$  sources for specific source areas during the months of January and February 1987. The source areas include: the Colorado river basin upslope to the continental divide; the Great Basin; the San Joaquin Valley; the southern coastal area of California; southern Arizona and northern Mexico; and western New Mexico including El Paso, Texas. Figure 6.4 shows the location of the sources and indicated their relative size. All coal fired power plants, smelters, and urban sources listed could impact the study area when the right meteorological conditions prevail.

### 6.2.2 $CD_4$ Emissions - Plume and Background measurements

A tracer, deuterated methane ( $CD_4$ ), was released from NGS's stacks during the WHITEX study.  $CD_4$  is a stable non-reactive species (even at elevated stack temperatures) and is presumed to have a deposition velocity close to zero. Table 6.2 presents the  $CD_4$  concentration measurements taken by aircraft. Samples were taken from the plume as well as upwind of NGS. Net concentrations were obtained by subtracting the background concentrations value of  $CD_4$  from the total

Table 6.1: Regional emissions in units of tons/day from coal fired power plants, copper smelter, and large urban areas. These values are based on annual data for 1987.

<u>SITE</u>	<u>LOCATION</u>	<u>SO<sub>2</sub></u>	<u>NO<sub>x</sub></u>	<u>PART</u>
Apache	Cohise, AZ	5.5	7.4	3.8
Coronado	St. Johns, AZ	17.5	19.2	.27
NGS	Page, AZ	163	73	6.4
Springerville	Springerville, AZ	13.2	10.1	.5
Cholla	Joseph City, AZ	44.7	35.9	4.4
Cameo	Grand Junction, CO	8.2	9.6	*
Craig	Craig, CO	24.4	38.4	*
Hayden	Hayden, CO	40.5	23.0	*
Escalante	Preuritt, NM	2.7	7.9	.4
Four Corners	Fruitland, NM	105.5	227.7	2.8
San Juan	Waterflow, NM	115.6	93.2	*
North Valmy	Valmy, NV	11.5	15.9	3.3
Mohave	Mohave, NV	51.5	42.2	*
Carbon	Castledale, UT	15.6	12.0	*
Hunter	Castledale, UT	15.9	53.4	*
Huntington	Huntington, UT	32.6	58.1	*
Bridger	Point of Rocks, WY	145.9	90.1	12.3
Naughton	Kemmerer, WY	41.4	40.3	*
Asarco-Hayden	Hayden, AZ	92	*	*
Inspiration	Miami, AZ	54	*	*
Magma	San Manuel, AZ	480	*	*
Nacozari	Nacozari, Sonora	380	*	*
Cananea	Cananea, Sonora	240	*	*
	LA/Southern CA	*	*	*
	Phoenix, AZ	*	*	*
	Las Vegas, NV	*	*	*
	El Paso, TX	*	*	*
	Salt Lake City, UT	*	*	*

Table 6.2:  $CD_4$  samples from NGS plume and upwind, units are ppt. Negative net values indicate that the total concentration was not significantly different from the background concentration of  $0.00027 \pm 0.00015$  ppt, the absolute value of the negative net values represents the upper concentration limits.

FLIGHT	DATE	TOTAL $CD_4$	NET $CD_4$
FLT 126 SRP SAMPLE	1/22/87	$0.00484 \pm 0.000469$	$0.00457 \pm 0.000493$
FLT 127 SRP SAMPLE	1/23/87	$0.004 \pm 0.000508$	$0.00373 \pm 0.000529$
FLT 128 PLUME-5 MI	1/29/87	$0.278 \pm 0.00357$	$0.278 \pm 0.00357$
FLT 128 PLUME-10 MI	1/29/87	$0.336 \pm 0.00558$	$0.336 \pm 0.00558$
FLT 128 PLUME-15 MI	1/29/87	$0.079 \pm 0.00124$	$0.0787 \pm 0.001250$
FLT 128 BKG SAMPLE	1/29/87	$0.000293 \pm 0.000125$	-0.000195
FLT 129 SRP SAMPLE	2/1/87	$0.00029 \pm 0.000188$	-0.00024
FLT 130 SRP SAMPLE	2/2/87	$0.00262 \pm 0.000407$	$0.00235 \pm 0.000434$
FLT 133 NGS PLUME?	2/13/87	$0.00113 \pm 0.000179$	$0.000858 \pm 0.000234$
FLT 133 NGS PLUME!	2/13/87	$0.030100 \pm 0.000889$	$0.0298 \pm 0.000902$
FLT 133 SRP SAMPLE	2/13/87	$0.005820 \pm 0.000399$	$0.00555 \pm 0.000427$
FLT 134 PLUME-5 MI	2/15/87	$0.308 \pm 0.00882$	$0.308 \pm 0.00882$
FLT 134 PLUME-10 MI	2/15/87	$0.209 \pm 0.00317$	$0.209 \pm 0.00318$
FLT 134 PLUME-15 MI	2/15/87	$0.104 \pm 0.00262$	$0.104 \pm 0.00263$
FLT 134 PLUME BKG	2/15/87	$0.0296 \pm 0.00192$	$0.0294 \pm 0.00193$

concentration. The background value was determined by acquiring pre-release samples on January 7 at Canyonlands and Bullfrog, the average of those values was 0.00027 ppt with a three standard deviation uncertainty of 0.00015 ppt. This is consistent with a global background value measured in Antarctica in 1984 of 0.0002 ppt.

The plume samples are identifiable by their elevated concentrations. For example, flight No. 128 on January 29 obtained three samples from the plume at a distance of 5, 10, and 15 miles downwind. At the 15 mile distance the concentration has decreased by over a factor of 3 to 0.079 ppt from the 10 mile sample which is 0.336 ppt. This can easily be explained by the plume diluting as it moves away from NGS. However, the concentration at the 5 mile distance, 0.278 ppt, is less than the 10 mile concentration. Because the sample uncertainties are low and the sampling time only minutes apart the difference between the 5 and 10 mile concentrations might be due to inhomogeneous mixing of the plume with the rest of the atmosphere. The plume samples obtained on January 29 and February 15, when approximately the same  $CD_4$  release rate was obtained, are quite similar to each other.

It is interesting to note that many of the upwind samples contain  $CD_4$  concentrations in excess of the global background concentration, by about a factor of 10. During stagnant periods, where the air sloshes back and forth in a diurnal pattern, it is possible the distribution of  $CD_4$  becomes ubiquitous in the immediate vicinity of NGS. The only upwind samples that were close to the global background were obtained on January 29 and February 1 immediately after the passage of a windy front on January 28 that cleaned out the atmosphere.

Table 6.3 summarizes measurements of trace elements, elemental sulfur,  $CD_4$ , and  $SO_2$  concentrations in the Navajo Generating Station plume by the airborne platform on 1/29/87 and 2/15/87. Other in-plume samples were gathered, however, sample loadings were too light to yield reliable elemental concentrations. Furthermore, the  $CD_4$  sample taken at 5 miles from NGS on 2/15/87 is

suspect because concentrations of  $SO_2$  and other trace elements associated with coal fired power plant emissions are higher at 5 miles while  $CD_4$  is lower as compared to the 10 mile sample. Again this could be due to inhomogeneous mixing of NGS plumes.

Table 6.4 presents the total sulfur ( $S$ )-to- $CD_4$ , total sulfur ( $S$ )-to-selenium ( $Se$ ) and selenium ( $Se$ )-to- $CD_4$  ratios measured in the plume by aircraft on both 1/29/87 and 2/15/87.  $CD_4$  concentrations are in parts per trillion, while  $SO_2$  is scaled to the elemental sulfur and added to elemental sulfur concentrations to yield total sulfur in  $\mu g/m^3$ .  $Se$  concentrations are also in  $\mu g/m^3$ . Since ambient  $CD_4$  concentrations were scaled to 2.5 mg/MWe-h,  $S/CD_4$ ,  $S/Se$  and  $Se/CD_4$  ratios with and without  $CD_4$  scaling are also shown in Table 6.4. Notice that while the  $S/Se$  ratios on both sampling periods are nearly the same the  $S/CD_4$  and  $Se/CD_4$  ratios are different by about a factor of two. This again could be due to the low  $CD_4$  concentration at 5 miles.

An independent method of checking the  $S/CD_4$  ratio is to calculate the ratio using known sulfur emissions as a function of  $MW_e$ . If it is assumed that there are  $1.72 \times 10^2 \mu g$  of sulfur per  $MW_e$  hr the  $S/CD_4$  ratio would be  $563 \mu g/m^3$  per ppt of  $CD_4$ . This is very close to the 540 ratio found in the 10 mile sample taken on 1/29/87. In the differential mass balance (DMB) calculations discussed in Section 6.6.2 the 540 ratio is assumed to be the correct ratio.

### 6.2.3 Scaling of $CD_4$ Data

An attempt was made to vary the tracer emission rate in proportion to the power plant load, i.e., emissions, to maintain a constant  $CD_4$  to  $SO_2$  ratio at NGS. However, the attempt to control the release rate was not particularly successful. The ratio of  $CD_4$  tracer to power plant load (and hence to emissions) was not constant but varied significantly around the average.

Due to this discrepancy in the  $CD_4$  releases, the  $CD_4$  data must be scaled or 'standardized' for a meaningful analysis. Using the release rate of 2.5 mg/MWe-h as a standard, Figure 6.5 shows the temporal history of the unscaled  $CD_4$  data, the  $CD_4$  release rate, and the scaled  $CD_4$  data at the Page receptor site. By comparing the scaled and unscaled  $CD_4$  time lines the action of the standardization can be seen; whenever the release rate increases above 2.5 the scaled  $CD_4$  values are reduced and vice versa. Many of the  $CD_4$  samples chosen for analysis occurred when the release rate was above 2.5 mg/MWe-h.

Since ambient levels of  $Se$  were above detectable limits for most of the sampling periods, and because  $Se$  is not expected to be chemically reactive with other atmospheric aerosol species, it is of interest to compare ambient ratios of  $Se$  and  $CD_4$  to those measured in the plume. Ambient selenium at Page was measured on a 12 hour schedule requiring that the 6 hour  $CD_4$  values be averaged to 12 hour values to facilitate the comparison. Figure 6.6 shows the scatter plot of  $Se$  and  $CD_4$  scaled to 2.5 mg/MWe-h for three different time periods that  $CD_4$  was released from different stacks or units at the Page monitoring site between JD = 27.33 thru JD = 45.33. From JD = 27.33 to JD = 37.3, tracer was released from Unit 1. From JD = 37.6 to JD = 41.3, Unit 1 was down and the release was from Unit 3. For JD = 41.3 to JD = 45.3, the release was switched back to Unit 1.

An examination of Figure 6.6 suggests that the relationship between  $Se$  and  $CD_4$  is dependent on which stack  $CD_4$  was released from. The dashed lines show the upper and lower  $Se/CD_4$  ratios measured in the plume on 1/29/87 and 2/15/87 while the slope of the dotted line, corresponding to the slope of  $Se/CD_4$  on days when  $CD_4$  was released out of Unit 3, is approximately 0.025.

Any  $Se/CD_4$  ratios greater than plume ratios could correspond to  $Se$  being transported into the area and not associated with NGS emissions. However, ambient  $Se/CD_4$  ratios associated with Unit 3 release correspond to  $CD_4$  apparent release rates that are about a factor of three higher than other time periods. Since there were no other sources of  $CD_4$ , the most likely explanation is

Table 6.3: Concentration of  $CD_4$  (ppt),  $SO_2$  ( $ng/m^3$ ), and trace elements ( $\mu g/m^3$ ) found in the Navajo Generating Station plume.

Date	1/29/87	2/15/87
Distance from NGS	10 miles	5 miles
$CD_4$ (ppt)	0.336	0.308
$SO_2$ ( $\mu g/m^3$ )	$430.6 \pm 43$	$717.7 \pm 72$
$Cu$ ( $ng/m^3$ )	$8.6 \pm 2$	$21.3 \pm 4$
$Zn$ ( $ng/m^3$ )	$13.6 \pm 2$	$17.2 \pm 2$
$Se$ ( $ng/m^3$ )	$27.2 \pm 5$	$38.2 \pm 10$
$Al$ ( $ng/m^3$ )	$380.0 \pm 29$	$400.0 \pm 28$
$Si$ ( $ng/m^3$ )	$663.0 \pm 69$	$709.0 \pm 65$
$S$ ( $ng/m^3$ )	$161.0 \pm 13$	$162.0 \pm 14$
$K$ ( $ng/m^3$ )	$36.0 \pm 16$	$31.0 \pm 15$
$Ca$ ( $ng/m^3$ )	$329.0 \pm 27$	$324.0 \pm 27$
$Ti$ ( $ng/m^3$ )	$29.0 \pm 9$	$20.0 \pm 8$
$Mn$ ( $ng/m^3$ )	$5.6 \pm 1.5$	$6.0 \pm 2$
$Fe$ ( $ng/m^3$ )	$197.0 \pm 11$	$197.0 \pm 11$
$Ni$ ( $ng/m^3$ )	$3.6 \pm 1.5$	$4.5 \pm 1.5$
$Sr$ ( $ng/m^3$ )	$5.5 \pm 2$	$9.3 \pm 3$
$Zr$ ( $ng/m^3$ )	$18.0 \pm 8$	$12.0 \pm 5$
$As$ ( $ng/m^3$ )	< 5	< 5

Table 6.4: Total sulfur ( $SO_2/2 + SO_4/3$ ) to  $CD_4$ , total sulfur to  $Se$  and  $Se$  to  $CD_4$  ratios found in the NGS plume. Scaled data refers to scaling the  $CD_4$  release rate to 2.5 mg of  $CD_4$  to one megawatt-hour generated by NGS.

	Unscaled		Scaled	
	1/29/87	2/15/87	1/29/87	2/15/87
	10 mi	5 mi	10 mi	5 mi
${}^a\text{Sulfur}/{}^b\text{CD}_4$	640	1164	540	1200
Sulfur/ ${}^c\text{Se}$	7900	9390	n/a	n/a
$\text{Se}/{}^b\text{CD}_4$	0.080	0.124	0.067	0.128

a.  $S = .5(SO_2) + (.333)SO_4$  ( $\mu g/m^3$ )

b.  $CD_4$  (ppt)

c.  $Se$  ( $\mu g/m^3$ )

## PAGE CD4

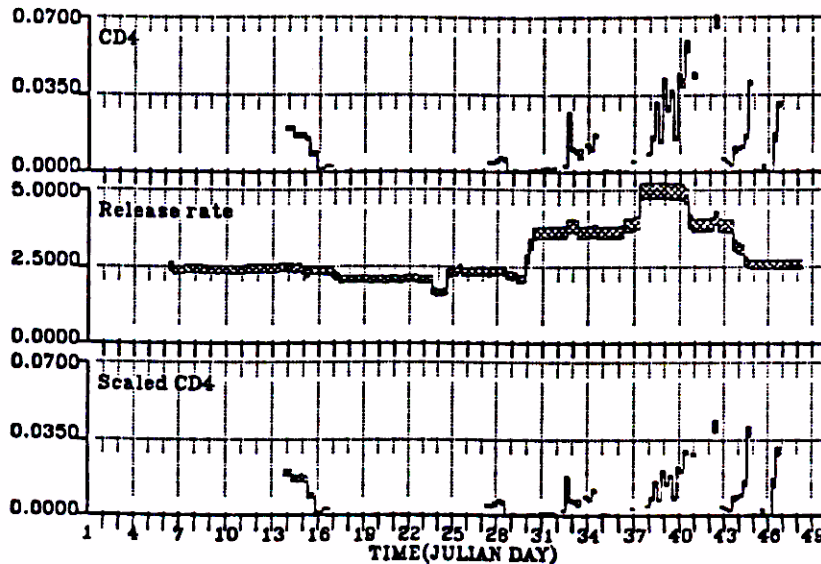


Figure 6.5: Raw  $CD_4$  concentrations (ppt),  $CD_4$  release rate (mg/MWe-h), and  $CD_4$  (ppt) scaled to release rate.

that the release rate from JD = 37.8-40.8 (Unit 3) was indeed higher. The ratio of the  $Se-CD_4$  slope corresponding to JD = 37.8-40.8 (Unit 3) and the lower bound of  $Se/CD_4$  measured in the plume is approximately 0.37; i.e.,  $0.025/0.067 = 0.37$ . Consequently, the  $CD_4$  release rate on JD = 37.8-40.8 is increased by a factor of  $2.7 = 1/0.37$  to account for Unit 3 tracer releases, the resulting  $Se-CD_4$  scatter plot for all data for JD = 27.3-45.3 appears as shown in Figure 6.7. The slope of the least square regression line is  $0.09220 \pm .01$  while the intercept =  $0.00027 \pm 0.00011$  ( $R^2 = 0.69$ ). For the time period corresponding to the high sulfate episode (JD = 37.8-45.3), the slope of the regression line is  $0.089 \pm 0.011$ , the intercept is not significantly different from zero, and  $R^2 = 0.85$ . The slope of either 0.092 or 0.089 is close to the average in-plume measured  $Se/CD_4$  ratio of 0.097 but somewhat higher than the best estimate of 0.067 found in the 10 mile 1/29/87 sample.

Figure 6.8 is temporal plots of ambient  $CD_4$  concentrations, the tracer release rate,  $CD_4$  scaled to NGS's emission rate, the apparent release rate accounting for Unit 3, and  $CD_4$  scaled to the apparent release rate, at the monitoring site for Page. The scaled  $CD_4$  data will be used for the remainder of this report.

## 6.3 Deposition and Transformation Rates

### 6.3.1 Dry Deposition Rates

Dry deposition is the process of mass transfer by which gases and particles are removed from the atmosphere to the surfaces of soil, rock, vegetation, and water bodies. Deposition involves a series of processes starting with atmospheric diffusion to the ground surface followed by various physical, chemical, and biological processes. Hicks<sup>1</sup> provides an excellent overview of the important processes